Frontiers in Offshore Geotechnics III – Meyer (Ed.)
© 2015 Taylor & Francis Group, London, ISBN: 978-1-138-02848-7

Predicting monopile behaviour for the Gode Wind offshore wind farm

F.C. Schroeder & A.S. Merritt
Geotechnical Consulting Group, London, UK

K.W. Sørensen, A. Muir Wood & C.L. Thilsted
DONG Energy, Gentofte, Denmark

D.M. Potts
Imperial College London, London, UK

ABSTRACT: Monopiles used as foundations for offshore wind turbines often have very large diameters and low length to diameter (L/D) ratios. Their response to lateral and moment loading is often modelled based on the API p-y method, although this was developed for slender piles with relatively small diameters. Theoretical studies and field monitoring have shown that this method may not accurately describe monopile behaviour, in particular the lateral load-displacement response for serviceability conditions. This paper presents advanced 3D Finite Element (FE) analyses undertaken during design of the Gode Wind offshore wind farm at a sand dominated site in the German North Sea. Two turbine locations with different soil profiles and varying monopile L/D ratios were analysed to compare the load-displacement and moment-rotation curves with the API p-y method. The FE analyses predict a stiffer response of the monopile from initial loading until the design ULS condition, which is consistent with field experience.

1 INTRODUCTION

Most current foundations used in the offshore wind industry are monopiles; stiff piles with large diameters, driven 20–35 m into the seabed. Recently installed monopiles have diameters of 5.5–6.5 m. In 2015 the Gode Wind offshore wind project will install larger still, 7.5 m diameter, monopiles in dense sands off the coast of Germany.

The current state-of-practice for design of monopiles in sand is to use p-y curves according to API (2011). These p-y curves have gained broad recognition due to the low failure rate of piles over several decades. However, when applied to offshore wind turbine foundations the design methodology is problematic for two main reasons:

Firstly, the p-y formulation is being used well beyond its verified range. The API p-y formulation for sand was originally adopted by Murchison and O'Neill (1983) on the basis of empirical data primarily obtained from two full-scale load tests reported by Cox et al. (1974) and the analysis presented in Reese et al. (1974). These tests were conducted using long, slender and flexible piles with diameter, $D = 0.61$ m and length, $L = 21$ m. In contrast, the next generation monopiles have diameters more than 10 times that. Furthermore, the L/D ratios will be in the range of 3–4 as opposed to the original pile tests where the L/D ratio was 34. It is therefore not reasonable to assume that the API p-y curves can accurately capture the response of large diameter monopiles with geometries much closer to suction caissons than traditional slender piles.

Secondly, critical design issues are not properly taken into account. It is characteristic for offshore wind turbines that the foundations are subjected to strong cyclic loading, originating from the wind and wave loads. This occurs not only during extreme conditions but also during serviceability conditions. Therefore, the primary design drivers for offshore wind turbine foundations are often those of deformation and stiffness rather than ultimate capacity. The API p-y curves are designed primarily for evaluation of the ultimate lateral capacity. Important design issues, such as accumulated rotation, effects of cyclic loading and small-strain stiffness are poorly accounted for.

Several numerical studies have been undertaken to investigate the behaviour of large diameter monopiles, see e.g. Augustesen et al. (2009), Lesny & Wiemann (2006) and Sorensen et al. (2010), however, conclusions tend to diverge. In contrast, results from full-scale measurements reported by Hald et al. (2009) and Kallehave et al. (2012) uniquely indicate that monopiles installed in sand behave significantly stiffer that predicted by API p-y curves.

The monopiles for Gode Wind offshore wind farm were designed using modified API p-y curves. 3D FE analyses were then used to benchmark and validate the geotechnical design in the serviceability and

ultimate limit states. This paper presents the 3D FE analyses and the results which were benchmarked to the modified API p-y curves for sand. The overall conclusion is that modified API p-y curves for sands still under-predict ultimate overturning capacities as well as small-strain stiffness in agreement with the reported full-scale measurements described above.

2 GODE WIND OFFSHORE WIND FARM

The Gode Wind offshore wind project is located in the German part of the North Sea 38 km north of the island of Norderney. The wind farm consists of 97 wind turbine generators, each with a rated power output of 6 MW.

The ground conditions at the project area are reasonably homogenous and typical for the German North Sea; the seabed consist mainly of dense to extremely dense Pleistocene sands (CPT q_c values of 50–110 MPa) with minor clay and silt layers spread across the site. A thin layer of post-glacial Holocene sediments comprising loose to very loose silty sands and medium dense to dense sand layers is present at the seabed overlying the Pleistocene strata. The water depths vary from 27.9–33.6 m and large wave loads are present at this North Sea site; the height of the 50-year extreme design wave is 18.5 m.

All foundations are driven monopiles (see Figure 1) with grouted transition pieces. Diameters are 6.5 m at turbine interface and 7.5 m at seabed. Each monopile was individually designed and optimised for the position specific loads and soil conditions. The monopile weights are in the range of 700–935 tonnes and can wall thickness' lie in the range of 70–100 mm. The penetration depths range from 24–32 m resulting in L/D ratios of 3.2–4.2.

The monopiles for Gode Wind were designed using modified API p-y curves. The major modifications included a) an un/reloading stiffness correction to ensure better prediction of as-built natural frequencies. The applied formulation was documented on the basis of as-built measurements from existing wind farms, b) addition of a toe-spring at the pile tip to account for low L/D ratios, c) lifetime accumulated deformations were calculated according to LeBlanc et al. (2010) while taking account of omni-directional loading and using model parameters derived for the site specific soil conditions and d) ultimate limit states were proofed against GEO-2 as required by DIN 1054:2010-12 while taking account for potential effects of cyclic degradations and pore pressure build-up during extreme storm events.

The monopile design for Gode Wind was governed by a combination of factors. The SLS criteria for accumulated lifetime deformations governed the pile length of most piles whereas the remaining piles were governed by the GEO-2 design proof. The pile diameter, and in some cases the can thickness, was governed by the un/reloading stiffness having a large effect on the natural frequency of the integrated foundation/turbine structure. The thickness of the remaining cans were governed by a combination of ultimate and fatigue limit states as well as robustness for installation.

Figure 1. Monopile for Gode Wind offshore wind farm (diameter = 7.5 m at seabed).

To validate the monopile designs based on the modified API p-y curves, 3D FE analyses were performed for two turbine locations with different ground conditions and varying L/D ratios. The analyses incorporated advanced soil models to accurately capture key features of the soil behaviour and determine the lateral load-displacement and moment-rotation response of the monopiles.

3 DETAILS OF THE 3D FE ANALYSES

3.1 *General*

The analysis of monopiles to lateral and moment loading requires the performance of 3D analyses. It is however possible to use one plane of symmetry at the centre of the pile in line with the direction of lateral load application, thus modelling only one half of the problem.

3D FE analyses were performed for turbine locations Q03 and H03. These locations were chosen, as the monopiles at locations Q03 and H03 are at the extreme ends of the L/D ratio spectrum across the site. For both locations the pile diameters below seabed were 7.5 m with a wall thickness of generally 75 mm. For location Q03, the penetration length considered in the analysis was 24.2 m, resulting in a L/D ratio of around 3.2, whereas for location H03 the penetration analysed was 35.1 m giving a L/D of approximately 4.7. Further design iterations at this location, for which no further FE analyses were carried out, allowed a reduction of the pile length resulting in a maximum L/D across the site of 4.2.

The loads applied to the monopile at each location were carefully derived considering extreme wave, current and wind loading. This resulted in a combination of horizontal and moment loads acting at the level of the seabed which is considered herein as the ULS load

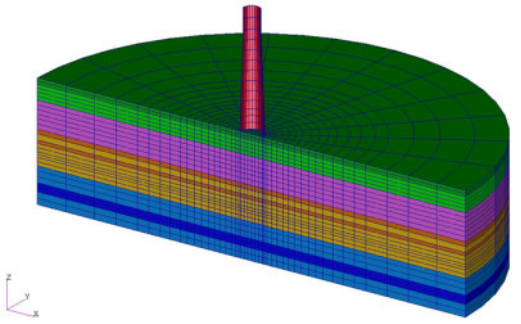

Figure 2. 3D FE mesh for analysis of Location Q03.

condition. In the FE model the structure above seabed was modelled up to a height that allowed the horizontal and moment load combination to be applied in a displacement controlled manner. For locations Q03 and H03, these were heights of 39.4 m and 41.4 m above seabed, respectively.

Figure 2 shows the FE mesh used for the analysis of location Q03. The overall dimensions of the mesh below seabed are given by a depth of 40 m and a radius of 75 m.

The analyses were performed using the FE code ICFEP. 20 node hexahedral elements were used in combination with 16 node interface elements (Day & Potts 1994) and 8 node shell elements (Schroeder et al. 2007). Reduced integration was used for all elements and a modified Newton-Rhapson scheme with an error controlled sub-stepping algorithm was employed as the non-linear solver (Potts & Zdravkovic 1999).

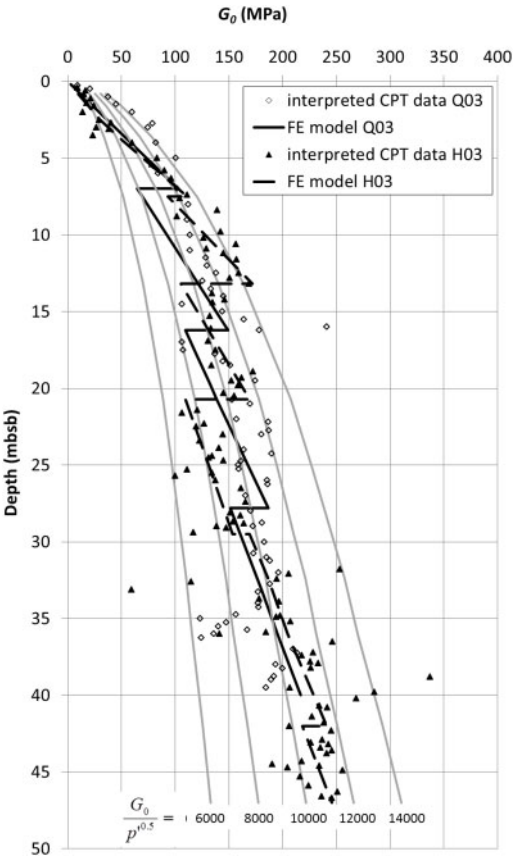

Figure 3. Variation of G_0 with depth – CPT data and FE model approximation (Location Q03).

3.2 *Geotechnical conditions and soil models*

The geotechnical conditions at each of the Gode Wind turbine locations were investigated by Cone Penetration Tests (CPTs), some with pore water pressure measurements, performed to 40–60 m below seabed. Some soil sampling and limited laboratory testing of the sands was also performed, including particle size distributions and index tests.

The basic geotechnical design profiles and parameters for the locations considered were derived principally from the CPT records and correlations with relative density and internal angle of shearing resistance. Internal angles of shearing resistance generally lay in the range of 35–42°.

In order to accurately model the stiffness-strain response of the sands, it is necessary to account for the pre-yield variation of soil stiffness with strain level, particularly at small strains, and the dependency on the stress level. Consequently, the sands were modelled as non-linear elastic perfectly plastic materials using a Mohr-Coulomb yield surface with non-associated plasticity, conservatively assuming an angle of dilation equal to zero for all sand layers.

The stiffness of sands at very small strain levels (G_0) depends on the mean effective stress ($p\prime$) to the power of 'n'. This can be reasonably modelled assuming $n = 0.5$; however, when approaching yield at larger strains a value of $n = 1.0$ is more appropriate (e.g. Porovic & Jardine 1994). To estimate the G_0 profiles with depth below seabed, the CPT cone resistance (q_c) profiles where used with the following correlation (Jardine et al. 2005):

$$G_0 = \frac{q_c}{0.0203 + 0.00125\eta - 1.216\times10^{-6}\times\eta^2}$$

where

$$\eta = \frac{q_c}{\sqrt{P_a \sigma'_{v0}}}$$

with P_a being the absolute atmospheric pressure (100 kPa) and $\sigma\prime_{vo}$ being the free field vertical effective stress.

The variation of G_0 with depth below seabed determined from the CPT profile at both turbine locations is shown in Figure 3. Also shown are lines representing constant values of $(G_0/p\prime)^{0.5}$ and the distributions of G_0 with depth assumed in the FE analyses. It can be seen that the variation in stiffness between the two locations is relatively small.

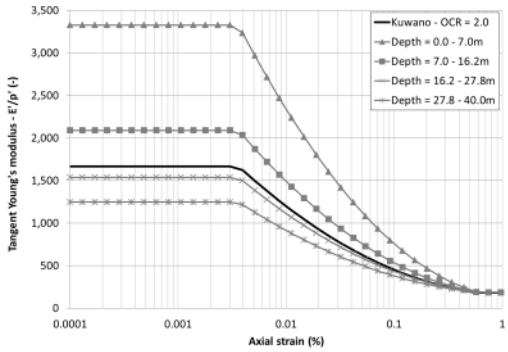

Figure 4. Stiffness-strain curves for different depths and strata (Location Q03).

The pre-yield constitutive model used in the analyses describes the variation of the normalised Young's Modulus (E'/p') with deviatoric strain in a manner similar to that proposed by Jardine et al. (1986). It assumes a constant Poisson's ratio of 0.25. Because the stiffness in the model is normalised directly by p' (rather than $p'^{0.5}$), different stiffness-strain relationships were used for different depths and soil layers, resulting in the stepped profile of stiffness with depth shown in Figure 3.

The stiffness-strain curves adopted for different depths and soil layers at location Q03 are shown in Figure 4. The shape of these curves was based on the idealised curve from an undrained triaxial test on North Sea sand from Dunkirk with an overconsolidation ratio of 2.0 (Kuwano 1999). The small strain stiffness values for each curve are based on the profile shown in Figure 3, and all curves converge to a similar normalized stiffness for axial strains greater than about 0.5%.

The interface between the monopile and the surrounding soil was modelled using specially formulated interface elements (Day & Potts 1994) with a Mohr-Coulomb yield surface and non-associated plasticity. Based on the average grain size (d_{50}) obtained from the available grain size distribution curves and published correlations (API 2011 and Jardine et al. 2005) an angle of interface friction of 29° was considered to be appropriate for all strata.

4 KEY RESULTS OF THE ANALYSES

4.1 *Load-displacement response*

The 3D FE analyses at locations Q03 and H03 were used to benchmark and validate the geotechnical design carried out using the modified API p-y methodology in the serviceability and ultimate limit states. This was achieved by comparing load-displacement and moment-rotation curves in terms of the ultimate capacity as well as the initial stiffness.

Figure 5a) shows the normalised load-displacement curves at seabed level for both locations up to lateral

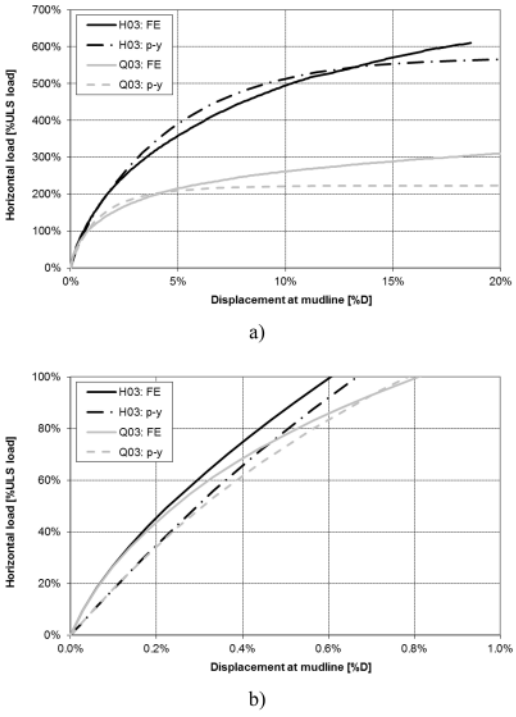

Figure 5. Load-displacement curves; comparison of FE and p-y.

displacements of around 0.2D, i.e. 1.5 m, comparing the results obtained from the FE analyses with those obtained from the modified p-y analysis. It can be seen that the predicted lateral load at these displacements for both analysis methods is well in excess of the design ULS condition.

For both locations the modified p-y analysis shows only small increases of lateral load at displacements approaching 0.2D, while the load obtained from the FE analyses are still increasing considerably. Furthermore, it should be noted that the assumption of zero dilation in the FE analyses is likely to significantly underestimate the ultimate capacity of monopiles in dense sands. As the measured behaviour of dense sands in the laboratory shows significant dilation, it is reasonable to expect a substantial increase in the resistance offered by the soil, particularly at the pile toe. Nonetheless, for displacements of around 0.2D, the FE analyses give lateral loads that are approximately 40% and 10% higher than the loads obtained from the corresponding p-y analyses for Locations Q03 and H03, respectively.

Figure 5b) gives a more detailed view of the initial part of the load-displacement curves enabling a comparison of the FE and p-y analyses results in terms of serviceability conditions. It is clear that the FE analyses predict a substantially stiffer response on initial loading than the modified p-y analyses. Lateral displacements obtained from the FE analyses at 10% of the ULS load are in the order of 50% of those

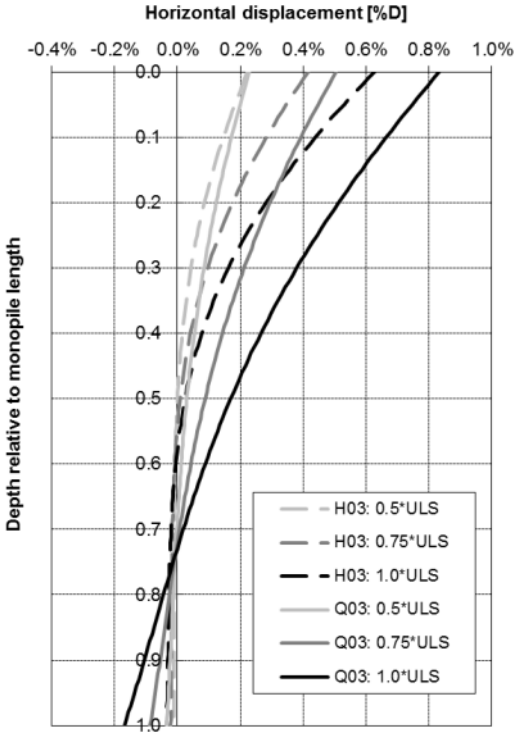

Figure 6. Horizontal pile displacement profiles during initial stages of loading.

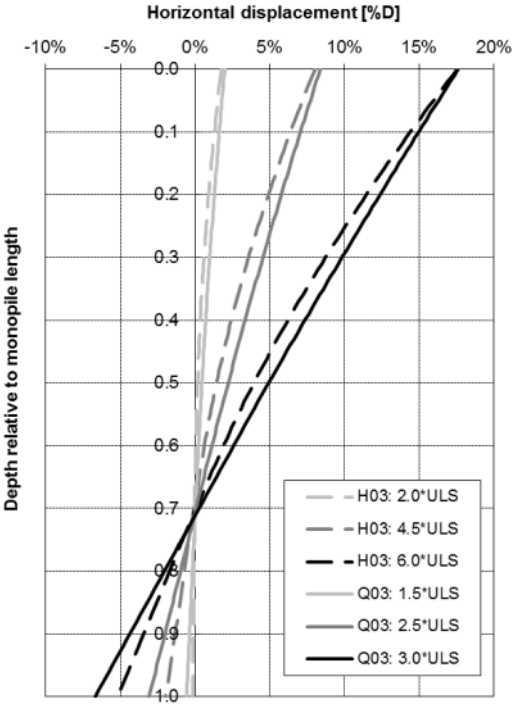

Figure 7. Horizontal pile displacement profiles approaching failure at 0.2D seabed displacement.

obtained from the modified p-y analyses indicating a substantially stiffer response of the monopiles under serviceability limit state loads. This agrees well with the findings from full-scale measurements reported by Hald et al. (2009) and Kallehave et al. (2012). It is interesting to note that the initial part of the load-displacement curve (up to around 25% of the ULS load) is very similar for both locations and does not appear to be significantly influenced by the difference in L/D ratio or soil profile. Given the relatively small areas of yield in the initial stages of loading, the assumption in terms of the angle of dilation is not significant in terms of the predicted pile response under operational load conditions.

Very similar conclusions, both in terms of the ultimate resistance and the serviceability conditions can be drawn for the moment-rotation behaviour. At the ULS loads, the analyses predict rotations at the seabed of approximately 0.3° and 0.25° for locations Q03 and H03, respectively.

4.2 *Displacement profiles and failure mechanisms*

Normalised horizontal displacement profiles with normalised depth below seabed for both locations are shown in Figures 6 and 7 for different load levels. It should be noted that similar seabed displacements for both locations are obtained for very different load levels, especially for larger loads. The figure clearly shows changing displacement profiles with increasing load levels. For small loads the monopiles are bending with only little backwards movement at the toe (toe kick). However, as the load level increases the piles increasingly rotate with increasing toe kick. For location Q03 toe kick commences for loads in excess of approximately half the ULS load whereas for Location H03 toe kick only commences for loads in excess of the ULS load.

For all load levels, the influence of the L/D ratio can be clearly seen with the shorter pile bending less than the longer pile. However, it is interesting to note that as failure is approached both monopiles rotate about a point at approximately 70% of their length.

The developing failure mechanism on the plane of symmetry is illustrated in Figure 8 by the incremental displacement vectors for Location Q03 at a load of around 3 times the ULS load. The overall lateral displacements at the seabed for this stage are in the order of 0.2D. Figure 8 indicates the following characteristic features of the likely ultimate failure mechanism in this plane:

1. Soil behind the pile “dropping” into the space opened up by the forward movement of the pile to significant depths;
2. Soil in the upper part in front of the pile is pushed sideways and upwards towards the seabed;
3. At depth, a rotational mechanism is developing.

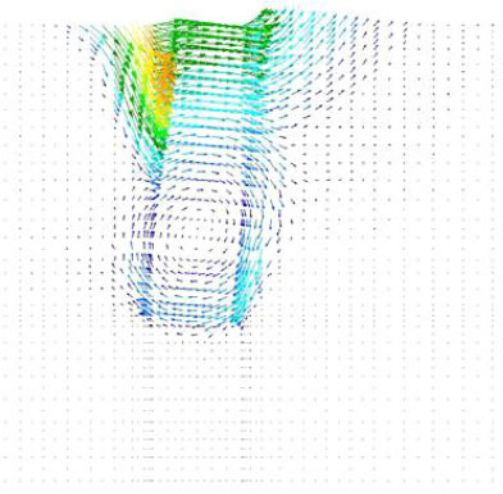

Figure 8. Incremental displacement vectors on the plane of symmetry for conditions approaching failure (Location Q03).

5 CONCLUSIONS

3D FE models were used to predict the behaviour of monopile foundations at selected locations of the Gode Wind offshore wind farm. The FE analyses used conservative parameters and incorporated advanced soil models to accurately represent the small-strain stiffness properties of the sands. The results indicate that the initial stiffness and ultimate capacity of low L/D ratio monopiles is significantly underestimated even when using a modified p-y approach. These FE models reinforce previously published observations from monitoring data that the API published methods are conservative for low L/D ratio piles. This conservatism remains even following modifications to the API p-y approach through the addition of a toe shear spring and increases in spring stiffness. The findings presented in this paper may indicate that additional springs are required to accurately model low L/D ratio piles in a simplistic manner.

For the offshore wind industry to continue to develop, the cost of design, construction and operation must continue to be reduced. The results from these FE analyses indicate that there remains further saving to be obtained through improved design methods.

REFERENCES

API. 2011. American Petroleum Institute (API) and International Organization for Standardization (ISO). *ANSI/API Specification RP 2GEO*. Geotechnical and Foundation Design Considerations for Offshore Structures.

Augustesen, A.H., Brodbaek, K.T., Moller, M., Sorensen, S.P.H., Ibsen, L.B., Pedersen, T.S. & Andersen, L. 2009. Numerical modelling of large-diameter steel piles at Horns Rev, *Civil Comp – CD Rom Edition*.

Cox, W. R., Reese, L. & Grubbs, B. R. 1974. Field testing of laterally loaded piles in sand. *Proc. Offshore Technology Conference*, Houston, Paper no. 2079.

Day, R.A. & Potts, D.M. 1994. Zero thickness interface elements – numerical stability and application. *Int. J. Numerical and Analytical Methods in Geomechanics,* Vol. 18, No. 10, 689–708.

DIN 1054:2010-12. 2010. *Baugrund – Sicherheitsnachweise im Erd- und Grundbau – Ergänzende Regelungen zu DIN EN 1997-1*.

Hald T., Morch C., Jensen L., Thilsted, C. & Ahle, K. 2009. Revisiting monopile design using p-y curves. Results from full scale measurements on Horns Rev, *Proc. European Offshore Wind*.

Jardine R.J., Potts D.M., Fourie A.B. & Burland J. B. 1986. Studies of the influence of non-linear stress-strain characteristics in soil-structure interaction. *Geotechnique,* Vol. 36, No. 3, 377–396.

Jardine, R.J., Chow, F.C., Overy, R. & Standing, J.R. 2005. *ICP Design Methods for Driven Piles in Sands and Clays*.

Kallehave, D., Thilsted, C. & Liingaard, M.A. 2012. Modification of the API p-y formulation of initial stiffness of sand. *Proc. 7th Int. Conf. Offshore Site Investigation and Geotechnics.* 465–472.

Kuwano, R. 1999. *The stiffness and yielding anisotropy of sand*. PhD Thesis University of London (Imperial College).

LeBlanc, C., Byrne, B.W. & Houlsby, G.T. 2010. Response of stiff piles to random two-way lateral loading *Géotechnique* 60 9: 715–721.

Lesny, K. & Wiemann, J. 2006. Finite-element-modelling of large diameter monopiles for offshore wind energy converters, *Geo-Congress 2006: Geotechnical Engineering in the Information Technology Age.*

Murchison, J.M. & O'Neill, M.W. 1984. Evaluation of p-y relationships in cohesionless soils. *Proc. Symp. Analysis and Design of Pile Foundations*, ASCE, San Francisco, 174–191.

Porovic, E. & Jardine, R.J. 1994. Some observations on the static and dynamic shear stiffness of Ham River sand. *Pre-failure Deformation of Geomaterials*.

Potts, D.M. & Zdravkovic, L.T. 1999. *Finite element analysis in geotechnical engineering – theory*, Thomas Telford Publishing, London, UK.

Reese, L.C, Cox, W.R. & Koop, F.D. 1974. Analysis of Laterally Loaded Piles in Sand. *Proc. 6th Offshore Technology Conference*, Paper no. 2080, Vol. 2, pp. 473–483.

Schroeder, F.C., Day, R.A., Potts, D.M. & Addenbrooke, T.I. 2007. A quadrilateral isoparametric shear deformable shell element for use in soil-structure interaction problems. *ASCE Int. J. Geomechanics,* Vol. 7, No. 1, 44–52.

Sorensen, S.P.H., Ibsen, L.B. & Augustesen, A.H. 2010. Effects of diameter on initial stiffness of p-y curves for large-diameter piles in sand. *Proc Numerical Methods in Geotechnical Engineering* – Benz & Nordal (eds), pp. 907–912